



HAL
open science

Quantitative image analysis of influence of polysaccharides on protein network formation in GDL-acidified milk gels

Mariska Brüls, Sanam Foroutanparsa, Théo Merland, C. Elizabeth P. Maljaars, Maurien M.A. Olsthoorn, Roderick P Tas, Ilja K Voets

► To cite this version:

Mariska Brüls, Sanam Foroutanparsa, Théo Merland, C. Elizabeth P. Maljaars, Maurien M.A. Olsthoorn, et al.. Quantitative image analysis of influence of polysaccharides on protein network formation in GDL-acidified milk gels. *Food Structure*, 2023, 38, pp.100352. 10.1016/j.foostr.2023.100352 . hal-04238300

HAL Id: hal-04238300

<https://hal.science/hal-04238300>

Submitted on 12 Oct 2023

HAL is a multi-disciplinary open access archive for the deposit and dissemination of scientific research documents, whether they are published or not. The documents may come from teaching and research institutions in France or abroad, or from public or private research centers.

L'archive ouverte pluridisciplinaire **HAL**, est destinée au dépôt et à la diffusion de documents scientifiques de niveau recherche, publiés ou non, émanant des établissements d'enseignement et de recherche français ou étrangers, des laboratoires publics ou privés.

1 **Quantitative image analysis of influence of polysaccharides on protein network formation**
2 **in GDL-acidified milk gels**

3 Mariska Brüls^{1,2}, Sanam Foroutanparsa^{1,2}, Théo Merland^{1,2}, C. Elizabeth P. Maljaars³,
4 Maurien M.A. Olsthoorn⁴, Roderick P. Tas^{1,2}, Ilja K. Voets^{1,2*}

5 ¹Laboratory of Self-Organizing Soft Matter, Department of Chemical Engineering and Chemistry, the
6 Netherlands

7 ²Institute for Complex Molecular Systems, Eindhoven University of Technology, P.O. Box 513, 5600
8 MB Eindhoven, the Netherlands

9 ³DSM Food & Beverages, Center for Food Innovation, Alexander Fleminglaan 1, 2613 AX Delft, The
10 Netherlands

11 ⁴DSM Science & Innovation, Biodata & Translational Sciences, Alexander Fleminglaan 1, 2613 AX
12 Delft, The Netherlands

13 *Corresponding author: i.voets@tue.nl

14

15

Abstract

16 Exopolysaccharides (EPS) are commonly used to improve the texture of yogurt. These
17 polysaccharides interact with casein micelles, the major protein in milk, via electrostatic and
18 depletion mechanisms during fermentation by lactic acid bacteria (LAB). However, the relationship
19 between the physicochemical properties and monosaccharide composition of EPS and their impact
20 on yogurt texture is not yet fully understood. To address this knowledge gap, we studied the effects
21 of polysaccharides commonly used as food additives on acid-induced milk protein networks. Confocal
22 laser scanning microscopy (CLSM) was used to image the network microstructures. Image analysis,
23 including Fourier transform, autocorrelation, and binarization-based techniques, was applied to
24 quantify key structural features of the mixed milk protein/polysaccharide gels. These parameters
25 were then related to the macroscopic properties of the model food matrices, such as elastic and
26 viscous moduli and yield point. We found that the addition of neutral polysaccharides resulted in a
27 concentration-dependent increase in structure factor, protein domain size, and pore fraction. In
28 contrast, the presence of charged polysaccharides led to an increase in protein domain size, a
29 decrease in pore fraction, and a decrease in elastic and viscous moduli. These results demonstrate
30 the use of a quantitative image analysis method for selecting LAB with favorable EPS properties to
31 improve yogurt texture.

32 **Keywords:** Acidified milk gel, polysaccharides, 2D spatial autocorrelation analysis, Fourier transform,
33 rheology

34

35 **1. Introduction**

36 The demand for healthy food products that are low-fat and free of synthetic additives has been
37 increasing due to the rising consumer awareness of the importance of good nutrition (Lynch et al.,
38 2018; Metilli et al., 2020). To meet these demands, the food industry must develop products that
39 offer improved nutritional and sensory quality. Achieving these requirements depends on an
40 understanding of the impact of ingredients on food microstructure and the resulting characteristics
41 of the final product (Aguilera, 2005). The microstructure is particularly critical in fermented milk
42 products, such as sour cream, cottage cheese, and yogurt. For these foods, the processing conditions
43 largely affect the final milk gel texture, firmness, and viscosity (John A. Lucey, 2004). Fermented milk
44 products are high in nutritional value and are consumed worldwide, with yogurt being the most

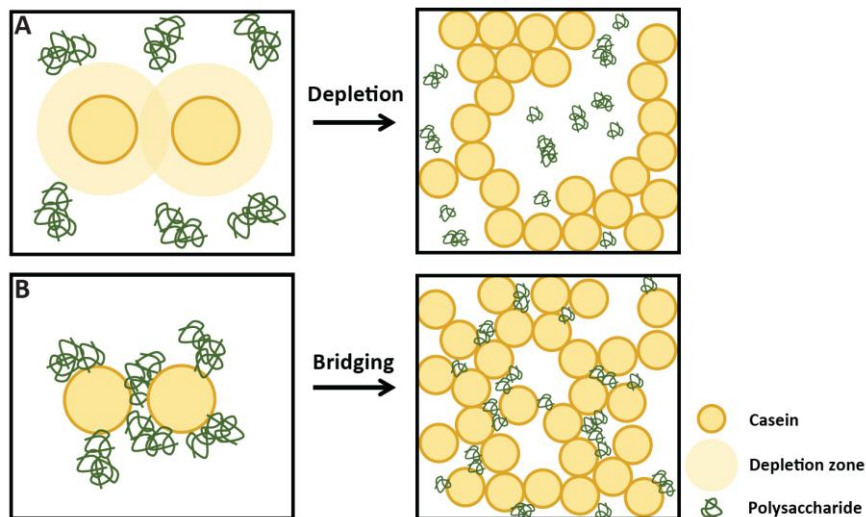
1 popular (Savaiano & Hutkins, 2021; Tamang et al., 2020). During the formation of yogurt, lactic acid
2 bacteria (LAB) convert lactose present in milk into lactic acid (Duboc & Mollet, 2001). The pH
3 decreases as a result, causing destabilization of the casein micelles, which comprise approximately
4 80% of the protein in bovine milk.

5
6 Casein micelles are assemblies of mainly four types of casein proteins (α_{s1} -, α_{s2} -, β -, and κ - caseins)
7 and colloidal calcium phosphate held together by hydrophobic interactions and hydrogen bonding
8 (Lucey & Singh, 1997). The κ -caseins are located on the outer surface of the micelles and stabilize the
9 casein micelles against aggregation by extending its hydrophilic C-terminal moiety, the so-called
10 caseinomacropeptide (CMP) (Dalgleish, 2011). The CMP is hydrophilic and extends away from the
11 casein micelle surface by 5-10 nm, creating a so-called 'hairy layer', which provides steric
12 stabilization. During acidification of milk, the CMP chains lose the intra- and interchain repulsive
13 electrostatic interactions and collapse onto the κ -casein layer (Dalgleish & Corredig, 2012). This
14 decreases the steric stabilization of the micelles, allowing them to aggregate by short-range
15 attractive forces, resulting in a sol-gel transition. The internal structure of the casein micelles also
16 changes upon acidification. When the pH decreases from 6.6 to 5.3, colloidal calcium phosphate
17 (CCP) is released from the interior of the micelles. A further decrease in pH to 4.6, corresponding to
18 the isoelectric point (pI) of caseins, results in aggregation and gelation. The microstructure of the
19 final yogurt network now consists of an aggregated casein protein network with embedded fat
20 globules and voids filled with serum with soluble proteins, lactose, bacterial cells and excreted
21 metabolites (Duboc & Mollet, 2001). The yogurt microstructure highly depends on the fermentation
22 process and the ingredient composition, and in turn the microstructure leads to specific physical and
23 sensory properties (Sodini et al., 2004). Therefore, it is important to understand how to tune yogurt
24 microstructure by optimizing the fermentation parameters.

25
26 An interesting aspect of LAB with regards to yogurt fermentation is the ability of certain LAB strains
27 to produce and secrete polysaccharides (Hassan, 2008). These polysaccharides include
28 exopolysaccharides (EPS) that are released into the surrounding medium and capsular
29 polysaccharides (CPS) that remain attached to the cell wall. Because of the diverse impact
30 polysaccharides have on the casein micelle network structure, EPS can be used to enhance yogurt
31 texture naturally without using additives. EPS can influence the formation of casein gels by
32 interfering with protein-protein interactions (Hassan, 2008), facilitate the formation of serum
33 channels and pores during gelation (Lynch et al., 2018), but also increase the compactness of the
34 casein network (Everett & McLeod, 2005) and either reduce (Zhang et al., 2016) or increase (Tiwari et
35 al., 2021) the water holding capacity.

36
37 The impact of a specific exopolysaccharide (EPS) on the microstructure of yogurt is influenced by
38 multiple factors, including monosaccharide composition, molecular mass, branching, stiffness, charge
39 density, and their interactions with milk proteins (Mende et al., 2016). Previous research on
40 commercially available polysaccharides has revealed general trends (Corredig et al., 2011; Syrbe et
41 al., 1998) and their underlying physical mechanisms (Kruif & Tuinier, 2001; Turgeon & Laneville,
42 2009), including their effects on network formation driven by depletion (Fig. 1A) or bridging (Fig. 1B).
43 Below the isoelectric pH of the caseins, anionic polysaccharides are attracted to the oppositely
44 charged casein micelles (now cationic), leading to bridging flocculation and destabilization of the
45 casein dispersions when the polysaccharide concentration is low. The compactness of the aggregates
46 increases with the number of protein-polysaccharide interactions, and denser structures can form
47 with higher numbers of opposite charges (Turgeon & Laneville, 2009). Electrostatic interactions with
48 anionic polysaccharides also strengthen the final protein network (Everett & McLeod, 2005) and
49 result in smaller pores (Loeffler et al., 2020). However, if the biomacromolecules have low affinity for
50 each other, the mixture may destabilize in a segregative manner through depletion, generating
51 domains enriched in either biomacromolecule and depleted of the other. This applies to mixtures of
52 neutral polysaccharides and casein micelles. Non-adsorbing neutral polysaccharides and excess

1 anionic polysaccharides increase serum viscosity (Everett & McLeod, 2005) and can accelerate casein
2 aggregation by depletion effects (Kruif & Tuinier, 2001). Stiffer polysaccharide chains may also
3 enhance protein aggregation. Rigid polysaccharides may bind weaker to oppositely charged
4 patches on the protein in an optimal manner (Kayitmazer et al., 2003). Laneuville and Turgeon
5 observed that xanthan and k-carrageenan, both having high chain stiffness, induce segregative phase
6 separation and induce syneresis in acidified milk gels (Laneuville & Turgeon, 2014). An increase in
7 branching (Tuinier et al., 2001) and charge density (Zdunek & Pieczywek, 2021) both increase the
8 stiffness of polysaccharide chains.
9
10



11
12 Figure 1. Schematic overview of polysaccharide/casein interaction modes and their consequences for
13 the formation and structure of milk protein gels. A) Non-adsorbing neutral and excess anionic
14 polysaccharides can drive casein aggregation by depletion flocculation. B) At low concentration
15 negatively charged, adsorbing polysaccharides can destabilize casein dispersions by bridging
16 flocculation. Adapted from de Kruif & Tuinier (Kruif & Tuinier, 2001).
17

18 Previous studies have investigated the interaction between milk proteins and a selection of specific
19 in-situ produced EPS (Ayala-Hernandez et al., 2008; Gentès et al., 2013), isolated EPS (Girard &
20 Schaffer-Lequart, 2008; Weinbreck et al., 2003) and polysaccharides (Buldo et al., 2016). However,
21 quantitative approaches have not yet been utilized to study the effect of EPS and polysaccharides on
22 the microstructure of mixed milk protein/exopolysaccharide gels. Several quantitative image analysis
23 techniques have been applied to yogurt microstructure, but these studies did not focus on the effect
24 of EPS and polysaccharides. Analysis techniques that have been utilized include grayscale
25 morphology analysis (Fenoul et al., 2008), typical aggregate size, binarization (Silva et al., 2015),
26 fractal image analysis (Torres et al., 2012), Fourier transform and autocorrelation based image
27 analysis (Glover et al., 2019) to assess various structural features of milk protein gels, such as fractal
28 dimension, protein domain size and pore fraction.
29

30 Since EPS produced by different LAB strains differ greatly in chemical composition and physical
31 properties (Birch et al., 2019), it is crucial to quantitatively analyze the microstructure of mixed milk
32 protein/exopolysaccharide gels to achieve a detailed, fundamental understanding of EPS structure-
33 yoghurt property relations. Whilst the rate and (local) concentration of LAB produced EPS is largely
34 unknown, it is important to investigate these properties for a comprehensive series of (E)PS
35 premixed with milk proteins, such that the composition of the milk protein/(exo)polysaccharide
36 mixtures is controlled and known. Whereas in previous work the effect of EPS on microstructure is
37 studied merely qualitatively, in this work we compare and contrast in a quantitative manner the
38 influences of different commercially-used polysaccharides, with known composition and physical

properties, on gelation in yogurt model systems, comprising mixtures of polysaccharides and milk protein concentrate powder (MPC) acidified by D-(+)-gluconic acid δ -lactone (GDL). We compared the effect on microstructure of polysaccharides that vary in charge density, hydrophilicity, chain flexibility and propensity to aggregate and form helices. Specifically, we focused on low acyl gellan (LAG), high acyl gellan (HAG), xanthan, guar gum and ι -carrageenan. We analyzed CLSM images from acidified milk gels containing these different types of polysaccharides to determine the structure factor, average protein domain size and pore fraction. This approach allows us to relate differences in microstructure induced by the various polysaccharides and imaged by CLSM to variations in the viscoelasticity of the network determined by rheometry.

2. Materials and Methods

2.1. Materials

Milk protein concentrate powder containing 80 wt% protein (MPC80) was kindly provided by the Hungarian Dairy Research Institute Ltd. During MPC80 powder preparation, milk was subjected to ultrafiltration and subsequent diafiltration to exclusively concentrate protein and casein-bound CaP (Babella, 1989). The retentate was heat treated by direct steam infusion at 130 °C for 20 seconds, followed by vacuum evaporation and spray-drying. The composition of the resulting MPC80 powder was 80% milk proteins (comprising a casein-to-whey protein ratio of 80:20, which is similar to the natural ratio in milk), 7.5% ash, 5.5% lactose, 5% water and 1.5% fat. LAG, HAG, xanthan, and yeast extract were kindly provided by DSM Biotechnology Center (Delft, The Netherlands). Guar gum, ι -carrageenan (commercial grade, type II), rhodamine B and D-(+)-gluconic acid δ -lactone (GDL, $\geq 99.0\%$) were purchased from Merck. Fresh pasteurized skimmed milk (fat content < 0.1%, de Zaanse Hoeve) was locally purchased in the Netherlands. All compounds were used as received. Characteristics of the commercially available polysaccharides used in this study, as reported in literature, are listed in table 1. A more extensive comparison of the properties of the polysaccharides, also based on information available from the literature, is given in the supplementary information (S1). In brief, low acyl gellan is produced from high acyl gellan by removal of the acetate and glycerate moieties (Buldo et al., 2016). HAG is less prone to aggregation compared to LAG since its acyl groups interfere with aggregation of double helices. As a result, LAG forms hard brittle gels whereas HAG forms soft elastic gels (Williams & Phillips, 2003). Xanthan has the same charge density as LAG and HAG but has a trisaccharide sidechain attached to every other monosaccharide unit in the backbone. Guar has a smaller, monosaccharide sidechain and is neutral, in contrast to ι -carrageenan which bears a negative charged sulphate group on every monosaccharide unit in the linear backbone.

Table. 1. Overview the PS and their composition, charge density and structure.

| Polysaccharide | Composition ^a | Molecular Weight (kg/mol) ⁱ | Persistence Length (nm) | Charge density ^a | Structure ^{b,c} |
|-----------------|---|--|-------------------------|-----------------------------|--------------------------|
| Low acyl gellan | Linear chain of glucuronic acid (◊), glucose (●) and rhamnose (▲) in the ratio 1 : 2 : 1. | $2.5 \cdot 10^2$ | 70-100 ^d | 0.25 | |

| | | | | | |
|-------------------------|---|------------------|---------|------|--|
| High acyl gellan | Linear chain of glucuronic acid with acetyl (OAc) and L-glyceryl as side-groups (Williams & Phillips, 2003), glucose and rhamnose in the ratio 1 : 2 : 1. | $1.5 \cdot 10^3$ | 25^e | 0.25 | |
| Xanthan | Glucose backbone with trisaccharide side-chain of mannose, glucuronic acid and mannose with acetyl and pyruvate (Pyr) substituents. | $1.5 \cdot 10^3$ | 125^f | 0.25 | |
| Guar | Mannose backbone with galactose (●) as monosaccharide side-chain. | $1.5 \cdot 10^3$ | 10^g | 0 | |
| ι-carrageenan | Linear chain of galactose and anhydrogalactose (Ⓢ), with a sulphate group (S) on every saccharide. | $1.5 \cdot 10^3$ | 23^h | 1 | |

1 ^a(de Jong & van de Velde, 2007), ^b(Cheng et al., 2017), ^cSchematically depicted using the standardized
2 Symbol Nomenclature For Glycans (SNFG). The configurations (α/β) and position of the glycosidic
3 linkages are indicated. ^d(Rinaudo & Milas, 2000), ^e(Jamil et al., 2019), ^f(Marguerite, 2001), ^g(Morris et
4 al., 2008), ^h(Schefer et al., 2014). ⁱMolecular weights (MW) of low acyl gellan and high acyl gellan
5 were determined by the supplier, the MW for xanthan, guar and ι -carrageenan were determined
6 from static light scattering as described in the supplementary information (S2).

7

8

9 2.2. Methods

10 2.2.1. Preparation of a GDL induced MPC80 gel

11 The yogurt model system was prepared based on the methods described by Zhang et. al. (Zhang et
12 al., 2015). MPC80 powder was reconstituted to 5.6 wt% (4.5 wt% protein) in MilliQ water and no
13 (control) or 0.04 wt% polysaccharide (LAG, HAG, xanthan, guar gum, ι -carrageenan) was added. This
14 concentration was selected since the protein network is continuous for all studied polysaccharides

1 up until this concentration (de Jong & van de Velde, 2007). The mineral content of the
2 polysaccharides, which is unknown, is assumed to be of negligible importance at this polysaccharide
3 concentration, which is much lower than the MPC concentration (with known mineral content). The
4 resulting reconstituted milk was heated in a thermomixer (Eppendorf® ThermoMixer® C) with mild
5 agitation (300 rpm) for 20 minutes at 90 °C and subsequently cooled in ice water for 30 minutes.
6 Sodium azide (0.02 wt%) was added as an antimicrobial agent and the protein was labelled with
7 rhodamine B (0.1 µg/ml), which binds strongly to proteins. The samples are equilibrated to room
8 temperature, subsequently 3.5 wt% GDL was added, and part of the sample was quickly transferred
9 to a chambered microscopy slide (chamber volume = 20 µl). Note that polysaccharide addition has a
10 negligible impact on the rate of pH decline (de Jong & van de Velde, 2007; Sone et al., 2022). As
11 determined by pH monitoring of the remaining sample volume, after incubation for 2 hours the pH
12 was 4.3, which below the pI of casein. At this time after GDL addition, five images of the final
13 network structure were taken per sample, and six repetitions are performed for each polysaccharide.
14 Therefore, for each polysaccharide a total of 30 images of milk gel microstructures are analysed.

15 2.2.2. Confocal laser-scanning microscopy

16 Confocal laser-scanning microscopy (CLSM, Leica SP8) was performed in the inverted mode with a
17 100x oil-immersion objective. The pixel size was set to 80 nm, using 0.75 digital zoom to generate
18 images of 1936 x 1936 pixels. Samples were excited with an incident laser at 552 nm with detection
19 between 565 and 630 nm. All images were taken >10 µm from the glass interface to avoid boundary
20 anomalies in the gel formation (Glover et al., 2019).

21 2.2.3. Quantitative data analysis

22 Analysis of variance (ANOVA) was used to evaluate differences between values of the protein domain
23 size, fractal dimension and pore fraction using multiple comparison of means Tukey Honest
24 Significant Difference (HSD) test. A significance level of $p < 0.05$ was used.

25 2.2.3.1. Pore fraction analysis

26 Prior to image analysis, the images are rescaled to maximize contrast using the automatic brightness
27 adjustment function in ImageJ. Further image analysis was conducted with Python 2 using inbuilt
28 functions for area calculation, Fourier transformation and additional custom-made functions. To
29 calculate the pore fraction, a wiener smoothing filter of 5 x 5 pixels was applied to the images using
30 the SciPy function 'wiener'. Inspired by the work of Pugnaroni et al. (Pugnaroni et al., 2005), images
31 were transformed into 8-bit binary images and thresholded, with the mean grey level as threshold. In
32 this way, any pixel with a grey level above the mean value is considered to belong to the protein
33 network, and any pixel with a grey level below is considered to belong to the voids within the
34 network. The pore fraction was subsequently calculated as the total pore area divided by the total
35 image area.

36 2.2.3.2. Autocorrelation and Fourier space analysis

37 The autocorrelation and Fourier space analysis were performed according to a method described by
38 Glover et al. (Glover et al., 2019). The autocorrelation $G(a,b)$ of an image is defined as:

$$G(a,b) = \sum_{x=1}^M \sum_{y=1}^N I(x,y) \cdot I(x-a,y-b) \quad (1)$$

39 Where M and N are the number of pixels in the height and width, respectively, (a,b) are the
40 coordinates in the generated autocorrelation image. According to the Wiener-Khinchin theorem

1 (Robertson, 2012), a computationally efficient method to compute the autocorrelation image is to
 2 take the inverse Fourier transform of the power spectrum image:

$$S(I) = |\mathcal{F}[I(x, y)]|^2 \quad (2)$$

$$G(a, b) = \mathcal{F}^{-1}[S(I)] \quad (3)$$

3 Where $S(I)$ is the power spectrum of the image, and \mathcal{F} represents the Fourier transform and \mathcal{F}^{-1} the
 4 inverse of the Fourier transform. The power spectrum describes how the signal is distributed over
 5 the spatial frequencies that together form the image. To limit the influence of variations in intensity
 6 over the samples, a normalized autocorrelation $g(a, b)$ is computed by subtraction of the mean
 7 intensity, and division by the standard deviation of the image:

$$g(a, b) = \frac{1}{\sigma(x, y)^2} \mathcal{F}^{-1}[\mathcal{F}[I(x, y) - \langle I(x, y) \rangle] \cdot \mathcal{F}^*[I(x, y) - \langle I(x, y) \rangle]] \quad (4)$$

8 Where $\sigma(x, y)$ is the standard deviation of the intensity values of the source image I , \mathcal{F}^* denotes the
 9 complex conjugate of the Fourier transform and $\langle I(x, y) \rangle$ is the average intensity in the image. Then,
 10 the radial distribution of the autocorrelation and power spectrum images are computed by a costum
 11 built python function which calculates for every pixel in the image the distance to the center of the
 12 image, and averages the correlation values over the pixels that have the same distance to the center.
 13 The radially averaged correlation values were normalized by division by the largest value, which is at
 14 the image center. As demonstrated by Ako et al. (Ako et al., 2009), the radially averaged
 15 autocorrelation decay can be fit to a stretched exponential:

$$p(r) = C \cdot e^{-\left(\frac{r}{\xi}\right)^\beta} \quad (5)$$

16 Where C is a constant, β is a value between 1 and 2, and ξ is the characteristic length which in this
 17 paper was taken as a measure of the protein domain size. The model $p(r)$ was fitted to the radial
 18 distribution of the autocorrelation image for each microscopy image using the function 'curve_fit' of
 19 the open-source Python library SciPy, and the value for the characteristic length ξ is extracted.

20 The structure factor was determined from the log-log plot of the radially averaged distribution of the
 21 power spectrum image $S(q)$. The power spectrum describes the distribution of power over the spatial
 22 frequencies that together form the image.

23

24 We assume the images can be described as an isotropic fractal Brownian surface (Super & Bovik,
 25 1991). For the global power spectrum of an isotropic fractal Brownian surface, the following relation
 26 in equation (6) applies:

27

$$S(q) \propto \left((u^2 + v^2)^{\frac{1}{2}} \right)^{-\beta} = q^{-\beta} \quad (6)$$

28

29 In which (u, v) are two-dimensional frequency coordinates, and the exponent $\beta > 0$ is the structure
 30 factor. Therefore, the gradient of the linear region in the $S(q)$ log-log plot is the structure factor β . To
 31 extract the structure factor β , a high order polynomial fit was applied to the $S(q)$ log-log plot and the
 32 minimum value of the derivative was taken as the slope $-\beta$ of the linear region.

33

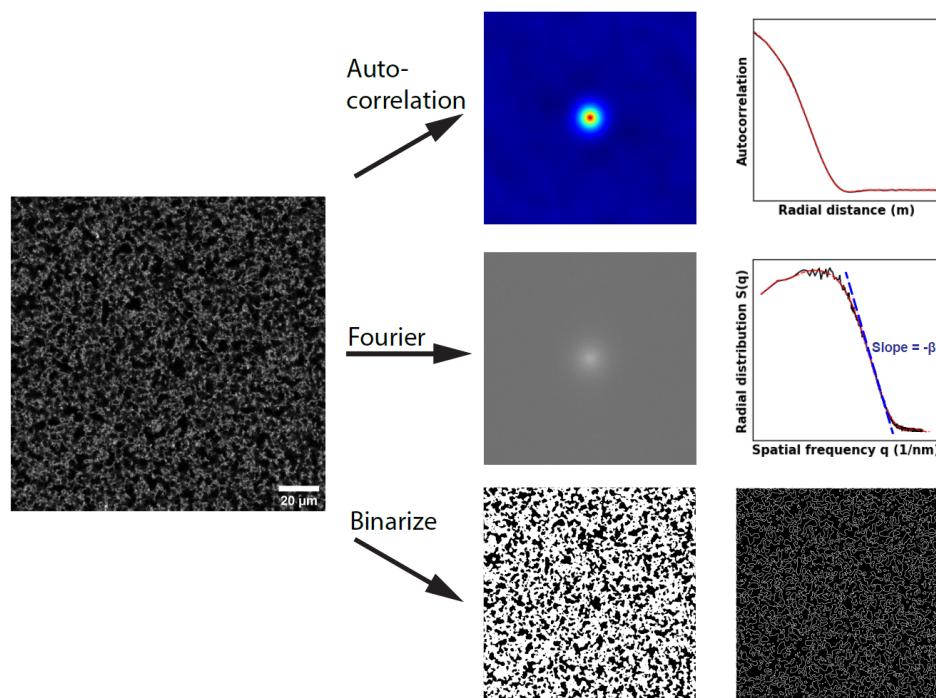
34 2.2.4. Rheology

35 Rheology measurements are performed with a rheometer (Anton Paar GmbH, MCR501) with double
 36 gap cylinder geometry (DG26.7-SN188610). GDL induced MPC80 gel samples with no (as a control) or

1 0.04 wt% polysaccharide (LAG, HAG, xanthan, guar gum or ι -carrageenan) were prepared as
 2 described in section 2.2.1. After storage overnight at 4 °C of the MPC80-polysaccharide samples, 3.5
 3 wt% D-(+)-gluconic acid δ -lactone (GDL, $\geq 99.0\%$, Merck) was added. Subsequently, 3.8 ml sample is
 4 added to the rheometer and a few oil droplets are added on top to prevent evaporation. After a 2
 5 hours waiting time to allow for gel formation at room temperature (20 °C) at rest, the rheological
 6 measurements were started. Frequency sweeps were performed across a frequency range of 100 to
 7 0.1 Hz at a constant strain of 1%. Amplitude sweeps were performed across a strain range of 1 to
 8 1000% at a constant frequency of 1 Hz. Each system was prepared twice and every prepared sample
 9 is measured once. The results are presented as the average of these two rheology measurements.

10 3. Results and discussion

11 Aiming to investigate the impact of polysaccharide properties and concentration on the
 12 microstructure of milk protein gels, GDL acidified samples were imaged using CLSM (see materials
 13 and methods). To quantify the influence of various polysaccharides and quantitatively compare
 14 differences in network structure, the CSLM images were subjected to an autocorrelation and Fourier
 15 space analysis as described by Glover et al. (Glover et al., 2019) (Fig. 2). These methods yield
 16 information on key features of the food matrices, such as protein domain size, pore fraction and the
 17 interfacial roughness of the gel strands in the network.



18
 19 Figure 2. Overview of the image analysis methods: (top) autocorrelation to calculate the average
 20 protein domain size, (middle) Fourier transformation to calculate the structure factor and (bottom)
 21 binarization to calculate the pore fraction and pore area distribution.

23 3.1. Microstructure of milk protein gels with commercially available polysaccharides

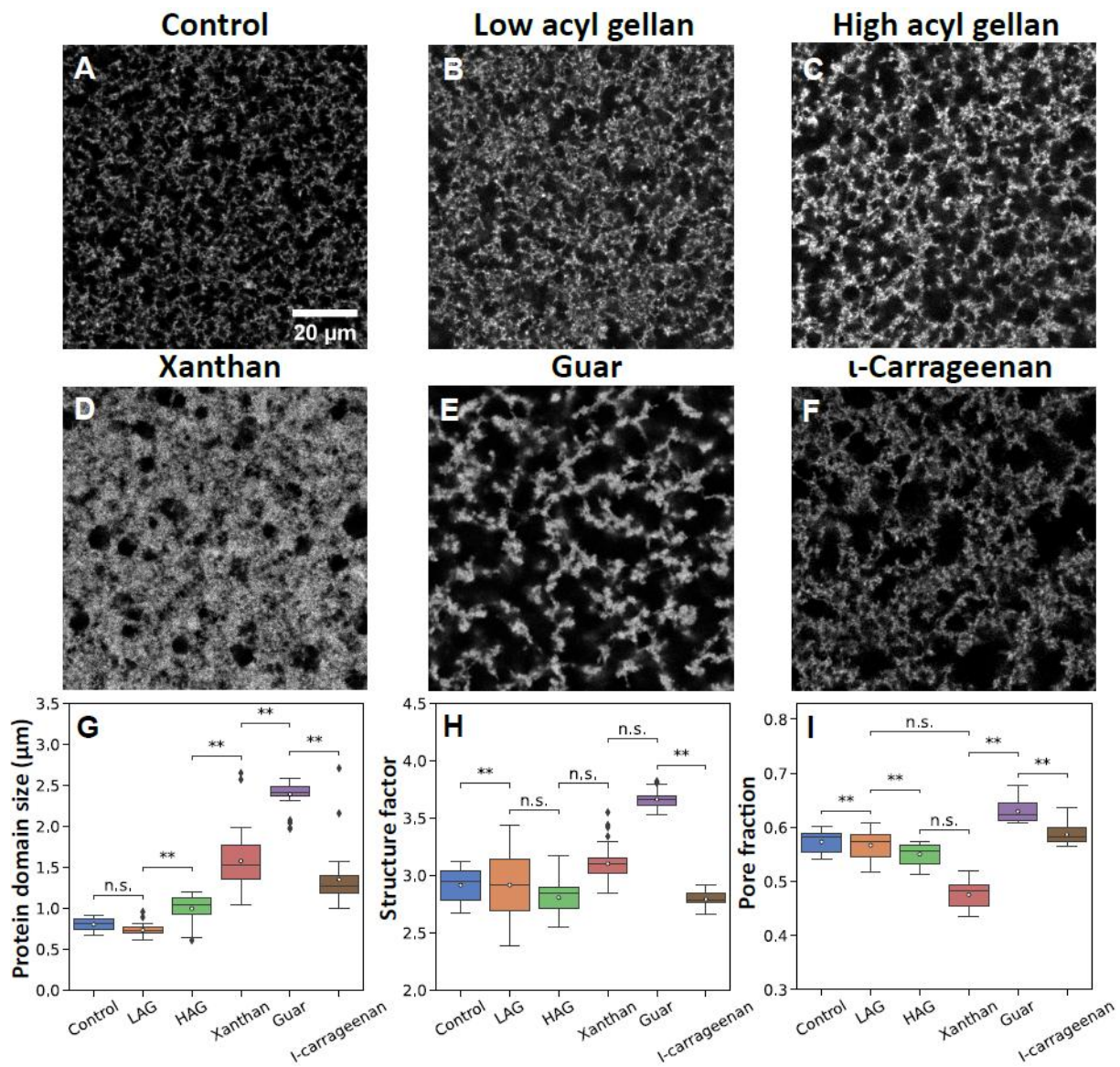
24 The network microstructures formed upon GDL acidification in the absence of PS or in the presence
 25 of one of LAG, HAG, xanthan, guar and ι -carrageenan have clearly different characteristics. While
 26 guar has a network with thick protein strands and large voids, the control has a network of fine
 27 protein strands and smaller void spaces. The networks with LAG and HAG have similar voids as the

1 control, but with thicker protein strands. The ι -Carrageenan network also has protein strands of
2 intermediate thickness, but larger voids. Finally, the xanthan network has a dense protein network
3 with both very small and large voids. This is apparent from both a qualitative inspection of the
4 confocal images (Fig. 3A-F) and from the quantitative analysis (Fig. 3-I). It is also in line with
5 observations on non-acidified renneted milk gel microstructures with 0.025wt% xanthan and guar
6 reported previously by others (Tan et al., 2007).

7 Quantitative analysis revealed significant differences in the microstructures of acidified milk with
8 different polysaccharides. Whilst the protein domain size of the milk protein networks without
9 polysaccharides (Fig. 3A) and with LAG (Fig. 3B) are statistically indifferent, the protein domain size
10 significantly increases ($PS \approx LAG < HAG < \iota$ -carrageenan < xanthan < guar) in the presence of all other
11 polysaccharides (Fig. 3G). These differences are not (easily) detectable upon an exclusively
12 qualitative inspection of the confocal images. Instead, quantitative analysis is required to uncover the
13 effect of added polysaccharides on the microstructure of model yoghurt networks. The protein
14 domains are on average largest in gels with guar and xanthan, with a far larger spread in strand
15 thickness in networks with xanthan than with guar. The mean strand thickness in mixed milk
16 protein/guar networks is about 2.5 μm . The average strand thickness of mixed casein/xanthan
17 networks is 1.7 μm , which is considerably lower. Intermediate protein domain sizes of approximately
18 1 and 1.4 μm are found in networks containing HAG and ι -carrageenan, respectively. None of the
19 analyzed protein domains in gels with HAG are as small as those without polysaccharides or in the
20 presence of LAG. Networks with ι -carrageenan comprise both small- and intermediate-sized
21 domains.

22 Gels with the neutral, non-adsorbing polysaccharide guar clearly stand out in protein domain size.
23 Both average domain size as well as the sizes of all analyzed domains were larger than the analyzed
24 domain sizes in all other gels, which do not contain neutral polysaccharides. We attribute this finding
25 to enhanced gel coarsening due to depletion interactions arising between the neutral guar and
26 charged casein micelles (Fig. 1A) (Kruif & Tuinier, 2001). In this scenario, it is thermodynamically
27 favorable to minimize the volume excluded to guar, so that its conformation entropy is least
28 compromised. Consequently, a depletion attraction arises between casein micelles, which effectively
29 pushes the milk proteins to aggregate and results in large protein domains interspersed by large
30 pores. Such a coarse microstructure increases the free volume accessible to the polysaccharides and
31 it is therefore entropically more favorable than a network with finer meshes. We observed a similar
32 effect for neutral EPS isolated from lactic acid bacteria, as described in the supplementary
33 information (S3).

34



1
2 Figure 3. Confocal images of the protein network microstructure of the GDL-induced milk gel: A)
3 control without polysaccharide, and B) with 0.04 wt% of low acyl gellan, C) high acyl gellan, D)
4 xanthan, E) guar and F) ι-carrageenan. Box plots of G) the protein domain size, H) structure factor
5 and I) pore fraction of the GDL-induced milk gels. Images were taken after 2 hours of incubation, at
6 pH 4.3. For samples, the number of images analyzed is n=30. Statistical significance as calculated with
7 multiple comparison of means Tukey HDS is indicated with asterisks, with not significant (n.s.) for
8 $0.05 < p < 1$, * for $0.01 < p < 0.05$ and ** for $0.001 < p < 0.01$.

9
10 Enhanced coarsening may also arise in the four networks containing negatively charged
11 polysaccharides due to bridging interactions at sufficiently low PS concentrations (Fig. 1B) or
12 depletion interactions (sufficiently high concentrations) at pH values below the pI of casein. The
13 branched, low charge density xanthan exhibits the largest impact on protein domain size of all
14 negatively charged PS investigated. Although we cannot directly and unambiguously relate specific
15 microstructural features to the characteristics of the polysaccharides, we believe that this finding is
16 in line with previous work by others showing xanthan having the stiffest chain conformation in milk
17 at neutral pH (Hege et al., 2020). Stiffer chains lead to stronger depletion attractions (Egorov, 2022).
18 Therefore, when present in excess, xanthan exhibits stronger depletion interactions with casein
19 micelles (partially) decorated with adsorbed xanthan chains resulting in enhanced coarsening. The
20 effect on protein domain size of ι-carrageenan is more pronounced than of LAG and HAG, but less

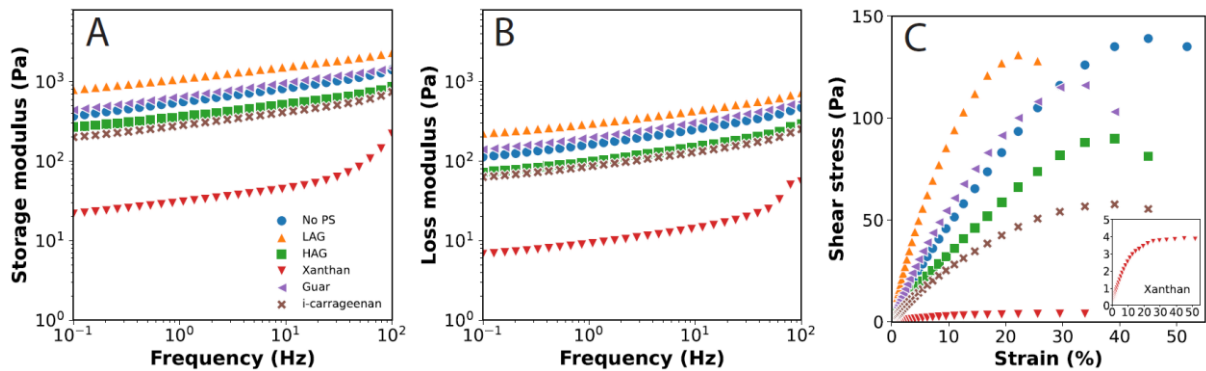
1 than that of guar and xanthan. As ι -carrageenan has both a high charge density (de Jong & van de
2 Velde, 2007) and a high degree of chain flexibility (Hege et al., 2020), this can likely be attributed to a
3 high level of bridging interactions. An insignificant impact on protein domain size is detected for the
4 linear, low charge density polysaccharide LAG, which may be related to the presence of less acyl
5 groups. Previous studies indicate that the presence of small side groups, such as acyl groups, can
6 interfere with PS-protein interactions (Buldo et al., 2016). Due to the larger number of acyl groups,
7 HAG may cause more depletion interaction than low acyl gellan. We propose that the coarser
8 network with larger protein domain size observed with HAG is due to stronger depletion interactions,
9 caused by the larger number of acyl groups compared to LAG.

10
11 Next, we analyzed the structure factor of the gels (Fig. 3H see section 2.2 for more information). The
12 structure factor is related and inversely proportional to the fractal dimension of the milk gels (Glover
13 et al., 2019). The milk gel microstructure can be modeled as a fractal Brownian surface, and based on
14 the definition of a fractal Brownian surface (Super & Bovik, 1991), a surface with smaller intensity
15 fluctuations, and thus a smoother surface, will have a larger fractal dimension, and thus a smaller
16 structure factor. Vice versa, a rougher surface results in a larger structure factor. Interestingly, it is
17 again the network with guar that stands out most. We find a structure factor of 3.67 ± 0.07 , which is
18 higher than that of all other gels without polysaccharide (value) or with anionic polysaccharides
19 (3.10 ± 0.14 , 2.91 ± 0.31 , 2.81 ± 0.13 and 2.79 ± 0.06 for xanthan, LAG, HAG and ι -carrageenan,
20 respectively. Hence, regardless of charge density, hydrophobicity, and branching density, the
21 microstructures in the presence of the negatively charged polysaccharides all display a comparatively
22 low structure factor. This suggests that the protein-serum interface is smoother in networks with
23 guar than on the other gels. The large spread in the structure factor of the LAG protein network is
24 notable and may be related to a more heterogeneous structure. The spread in domain size is not
25 much larger than for other mixed polysaccharide/milk protein gels (Fig. 3G), but we did observe
26 heterogeneously distributed regions with higher protein density. These correspond to markedly
27 brighter spots in the confocal images of the network. The different polysaccharides also impact the
28 porosity (Fig. 3I). Compared to all the other milk gels, the gels with guar are significantly more porous
29 (with $p < 0.01$) with a total pore fraction of 0.63 ± 0.02 . The large pore fractions in the milk gels with
30 guar are expected for a non-adsorbing neutral polysaccharide able to cause strong depletion
31 interactions. In a control experiment, no whey separation was observed in any of the gels, ruling out
32 that the smaller pore fraction of the other gels is due to whey separation (Supplementary Figure S2).
33 The pores in this network appear rather large and interconnected. The smallest pore volume fraction
34 is found in the presence of xanthan (0.48 ± 0.02), whilst all other gels with and without anionic
35 polysaccharides display comparable porosity with pore volume fraction of 0.55 ± 0.02 up to 0.59 ± 0.02 .
36 At neutral pH, xanthan-milk solutions at the composition used in this study are unstable and phase
37 separate (Hemar et al., 2001). However, the differences in pore fraction distributions among the
38 images of these gels were not statistically significant.

39 In summary, the mixed milk protein/polysaccharide network with the neutral polysaccharide guar
40 differs markedly in microstructure from the milk protein gels without polysaccharide and from those
41 with any of the four studied anionic polysaccharides. The guar gel is fairly dense, has a large pore
42 fraction and exhibits a rather smooth protein-serum interface. The negatively charged
43 polysaccharides have more subtle effects on protein domain size, fractal dimension and pore
44 fraction. Differences between these effects are too modest to be appreciated upon qualitative
45 inspection of the confocal images but do become distinguishable upon quantitative analysis.

46 47 48 *3.2. Rheological properties of milk protein gels with commercially available polysaccharides* 49

1 Next, we performed rheometry (Fig. 4) to probe viscoelasticity and yielding. In the linear domain (Fig.
 2 4A, B), all gels display elastic behavior ($G' > G''$) within the studied frequency range. Interestingly,
 3 most of the studied polysaccharides impact both G' (Fig. 4A) and G'' (Fig. 4B) in a similar manner. For
 4 a direct comparison of the moduli of the different milk gels, we focus on G' and G'' at 1Hz (Table 2).
 5 Whilst the presence of LAG induces an approximately two-fold increase in G' and G'' (to 1210 ± 45 and
 6 310 ± 5 Pa respectively) compared to the gel without polysaccharide (560 ± 6 and 160 ± 3 Pa), HAG and
 7 ι -carrageenan decreased the elastic modulus G' and the loss modulus G'' by a factor of 1-2. Sone et
 8 al. observed a similarly slight decrease in decrease in G' and G'' for GDL acidified milk gel with 0.05
 9 wt% ι -carrageenan (Sone et al., 2022). A marked decrease in both G' and G'' is seen upon addition of
 10 xanthan (36 ± 4 and 11 ± 1 Pa, respectively). Strikingly, the addition of guar only slightly increased G'
 11 and G'' , to 630 ± 50 and 190 ± 20 , whilst mixed milk protein/polysaccharide networks with this neutral
 12 polysaccharide display the most pronounced differences in microstructure. Tan et al. observed a
 13 larger increase in complex modulus for renneted skim milk gels with similar guar concentration (Tan
 14 et al., 2007).
 15
 16



17
 18 Figure 4. A) Storage modulus (G'), B) loss modulus (G'') as function of frequency and C) shear stress
 19 as a function of strain for GDL-induced milk gel without polysaccharide (blue circles), and with 0.04
 20 wt% of low acyl gellan (orange triangles pointing upwards), high acyl gellan (green squares), xanthan
 21 (red triangles pointing downwards), guar (purple triangles pointing to left) and ι -carrageenan (brown
 22 crosses).
 23

24 The observed trends in viscoelasticity persist in the non-linear rheology up to moderate strains of
 25 20 - 25% (Fig. 4C). Yield stress and strain were determined from these experiments, during which an
 26 increasingly strong strain was applied to the gels until these finally ruptured. Interestingly, the largest
 27 yield strain of $45 \pm 6\%$ and yield stress (140 ± 3 Pa) was found for the gels devoid of polysaccharide
 28 (Table 2). Hence, the addition of polysaccharides, neutral as well as anionic, reduces gel toughness
 29 and makes the networks more brittle instead. Apart from the gel network with LAG, which was stiffer
 30 than the control gel network, globally the control gels were weaker than the gels containing
 31 polysaccharides. LAG is known to form brittle gels and to disrupt at lower strain but higher stress
 32 compared to HAG gellan (Tong et al., 2018). It ruptured at the same yield stress (140 ± 7 Pa) but two-
 33 fold lower yield strain ($22 \pm 3\%$) than the control milk protein gel. In contrast, HAG did not significantly
 34 affect the yield strain, but reduced the yield stress to 84 ± 6 Pa. The milk gel with guar had similar yield
 35 stress and yield strain as the control milk gel. For xanthan, the yield stress decreased forty-fold to 3
 36 Pa at 28% strain. These findings agree with the reduction in complex modulus for milk gels with
 37 0.025-0.1 wt% xanthan compared to skim milk without polysaccharide, as observed by Tan et al. (Tan
 38 et al., 2007). They also observed that xanthan tended to slow down gelation and caused formation of
 39 a discontinuous protein network, which likely explains the lower G' and G'' . At the composition used
 40 in our study, 0.04wt% and 4.5 wt% milk protein, the xanthan-milk mixture was already
 41 thermodynamically incompatible and ready to phase separate at neutral pH (Hemar et al., 2001).
 42

1 Table. 2. Rheological properties of the milk gels: Storage modulus and loss modulus at 1 Hz and 1% strain, and
 2 the yield stress and yield strain. All measurements were performed in duplicate; the reported values denote
 3 the mean with accompanying standard deviation.

| Polysaccharide | Storage modulus (Pa) | Loss modulus (Pa) | Yield Stress (Pa) | Yield strain (%) |
|--------------------------|-----------------------------|--------------------------|--------------------------|-------------------------|
| No polysaccharide | 560±6 | 160±3 | 140±3 | 45±6 |
| Low acyl gellan | 1210±45 | 310±5 | 140±7 | 22±3 |
| High acyl gellan | 390±2 | 110±7 | 84±6 | 39±6 |
| Xanthan | 36±4 | 11±1 | 3±0.5 | 28±10 |
| Guar | 630±50 | 190±20 | 130±10 | 40±6 |
| ι-carrageenan | 270±40 | 83±10 | 50±10 | 34±5 |

4
5
6

3.3. Relation between rheological properties, gel microstructure and polysaccharide properties

7 The small yet detectable differences in rheological properties of the mixed polysaccharide/milk
 8 protein gels are related in a complex manner to subtle variations in microstructure which in turn
 9 originate from differences in the interactions between the various integrated polysaccharides and
 10 milk proteins. Although no unambiguous trends were observed between the differences in
 11 microstructure and rheological properties, the observations in this study can serve as the basis of
 12 future hypotheses on microstructure-function relationships in yogurt. Xanthan does not reinforce the
 13 protein network, but rather appears to hinder protein-protein interactions that are essential for the
 14 formation of a strong and tough milk protein gel. The low moduli for xanthan-containing gels have
 15 been related before to a decrease in the continuity of the protein phase; an effect that becomes
 16 more pronounced with increasing polysaccharide concentration (de Jong & van de Velde, 2007).
 17 Whether the low moduli are also related to the rather low pore volume fraction is still to be
 18 uncovered. The low pore fraction does not seem to be caused by syneresis, since no syneresis was
 19 observed (Supplementary information S4). The larger G' and G'' values and brittleness of the low acyl
 20 gellan gel are possibly related to its strong interaction with calcium ions (Sworn & Stouby, 2021) and
 21 casein (Buldo et al., 2016). and to the presence of non-uniformly distributed dense protein domains,
 22 which give rise to the large spread in structure factor. High acyl gellan and ι-carrageenan have similar
 23 G' and G'' , protein domain size and structure factor. Arguably most striking is the similarity in
 24 rheological properties of the gel without any polysaccharide and the guar gel, while their
 25 microstructures greatly differ. The guar gel has slightly yet significantly higher moduli than the
 26 pristine gel, has a higher porosity, a larger structure fraction and a larger protein domain size. These
 27 microstructural differences may have opposing effects on the rheological properties, such that their
 28 combined effect is small. Alternatively, their impact may be attenuated by other factors such as the
 29 increased guar concentration in the serum due to depletion-induced phase separation in these
 30 mixtures comprising neutral polysaccharides and milk proteins. Similarly, van der Velde et al.
 31 observed significant differences in whey-gel microstructure at 0 and 0.05 wt% guar, yet at this
 32 concentration the guar had little impact on Young modulus (de Jong & van de Velde, 2007).
 33 Interestingly, they observed the highest Young modulus at a guar concentration when the pore
 34 fraction is largest. To conclusively relate the microstructure characteristics to the rheological
 35 properties, the present study could be extended to different polysaccharide concentrations.

36
37

5. Conclusions

38 The influence of different polysaccharides on the microstructure and rheological properties of yogurt
 39 model systems has been quantified in mixtures of food grade polysaccharides and milk protein
 40 concentrate acidified by GDL. The addition of polysaccharides with varying composition, charge

1 density and branching density resulted in milk gels with distinct microstructures and rheological
2 properties. Quantitative image analysis of CLSM images of these acidified milk gels yielded the
3 structure factor, average protein domain size and pore fraction as parameters to describe the key
4 features of the microstructure. Through this multi-parameter, quantitative image analysis approach,
5 the influence of various polysaccharides on the milk gel microstructure could be differentiated, even
6 if these were not directly apparent from visual inspection by eye. We found that the addition of the
7 neutral polysaccharide guar had the least impact on the rheological properties of the acidified milk
8 protein gels even though these networks have a larger structure factor, larger protein domain size
9 and larger pore fraction compared to networks with negatively charged polysaccharides. Subtle
10 differences in microstructure were detectable in networks containing different negatively charged
11 polysaccharides, presumably originating from variations in their interactions with the milk proteins in
12 the gels. A high degree of acylation, high branching density and high charge density increased protein
13 domain size and weakened the gel network. In future, the presented methodology can also be
14 employed in time-resolved studies to monitor the development of the microstructure and
15 rheological properties of the network. This would reveal when the gels in the presence and absence
16 of various polysaccharides develop characteristic differences and how their formation pathways
17 relate to the final network microstructures and their rheological properties. Another interesting
18 avenue of future research is multi-color imaging of mixed gels with both the proteins and
19 polysaccharides specifically labelled to elucidate the extent to which these are locally mixed and how
20 this relates to network structure and properties.

21 **Acknowledgements**

22 This publication is part of the project Localbiofood (with project number 731.017.204) of the
23 research program Science PPP Fund, which is (partly) financed by the Dutch Research Council (NWO)
24 in collaboration with ChemistryNL. We would like to thank our colleagues in the LocalBioFood
25 consortium for the fruitful discussions.

26 **References**

- 27 Aguilera, J. M. (2005). Why food micro structure? *Journal of Food Engineering*, *67*(1–2), 3–11.
28 <https://doi.org/10.1016/j.jfoodeng.2004.05.050>
- 29 Ako, K., Durand, D., Nicolai, T., & Becu, L. (2009). Quantitative analysis of confocal laser scanning
30 microscopy images of heat-set globular protein gels. *Food Hydrocolloids*, *23*(4), 1111–1119.
31 <https://doi.org/10.1016/j.foodhyd.2008.09.003>
- 32 Ayala-Hernandez, I., Goff, H. D., & Corredig, M. (2008). Interactions between milk proteins and
33 exopolysaccharides produced by *Lactococcus lactis* observed by scanning electron microscopy.
34 *Journal of Dairy Science*, *91*(7), 2583–2590. <https://doi.org/10.3168/jds.2007-0876>
- 35 Babella, G. (1989). Scientific and practical results with use of ultrafiltration in Hungary. *International*
36 *Dairy Federation*, *244*, 7–24.
- 37 Birch, J., Van Calsteren, M. R., Pérez, S., & Svensson, B. (2019). The exopolysaccharide properties and
38 structures database: EPS-DB. Application to bacterial exopolysaccharides. *Carbohydrate*
39 *Polymers*, *205*(October 2018), 565–570. <https://doi.org/10.1016/j.carbpol.2018.10.063>
- 40 Buldo, P., Benfeldt, C., Carey, J. P., Folkenberg, D. M., Jensen, H. B., Sieuwerts, S., Vlachvei, K., &
41 Ipsen, R. (2016). Interactions of milk proteins with low and high acyl gellan: Effect on
42 microstructure and textural properties of acidified milk. *Food Hydrocolloids*, *60*, 225–231.
43 <https://doi.org/10.1016/j.foodhyd.2016.03.041>
- 44 Cheng, K., Zhou, Y., & Neelamegham, S. (2017). DrawGlycan-SNFG: A robust tool to render glycans

- 1 and glycopeptides with fragmentation information. *Glycobiology*, 27(3), 200–205.
2 <https://doi.org/10.1093/glycob/cww115>
- 3 Corredig, M., Sharafbafi, N., & Kristo, E. (2011). Polysaccharide-protein interactions in dairy matrices,
4 control and design of structures. *Food Hydrocolloids*, 25(8), 1833–1841.
5 <https://doi.org/10.1016/j.foodhyd.2011.05.014>
- 6 Dalgleish, D. G. (2011). On the structural models of bovine casein micelles - Review and possible
7 improvements. *Soft Matter*, 7(6), 2265–2272. <https://doi.org/10.1039/c0sm00806k>
- 8 Dalgleish, D. G., & Corredig, M. (2012). The Structure of the Casein Micelle of Milk and Its Changes
9 During Processing. *Annual Review of Food Science and Technology*, 3(1), 449–467.
10 <https://doi.org/10.1146/annurev-food-022811-101214>
- 11 de Jong, S., & van de Velde, F. (2007). Charge density of polysaccharide controls microstructure and
12 large deformation properties of mixed gels. *Food Hydrocolloids*, 21(7), 1172–1187.
13 <https://doi.org/10.1016/j.foodhyd.2006.09.004>
- 14 Duboc, P., & Mollet, B. (2001). Applications of exopolysaccharides in the dairy industry. *International*
15 *Dairy Journal*, 11(9), 759–768. [https://doi.org/10.1016/S0958-6946\(01\)00119-4](https://doi.org/10.1016/S0958-6946(01)00119-4)
- 16 Egorov, S. A. (2022). Depletion Interactions between Nanoparticles: The Effect of the Polymeric
17 Depletant Stiffness. *Polymers*, 14(24). <https://doi.org/10.3390/polym14245398>
- 18 Everett, D. W., & McLeod, R. E. (2005). Interactions of polysaccharide stabilisers with casein
19 aggregates in stirred skim-milk yoghurt. *International Dairy Journal*, 15(11), 1175–1183.
20 <https://doi.org/10.1016/j.idairyj.2004.12.004>
- 21 Fenoul, F., Le Denmat, M., Hamdi, F., Cuvelier, G., & Michon, C. (2008). Technical note: Confocal
22 scanning laser microscopy and quantitative image analysis: Application to cream cheese
23 microstructure investigation. *Journal of Dairy Science*, 91(4), 1325–1333.
24 <https://doi.org/10.3168/jds.2007-0531>
- 25 Gentès, M. C., St-Gelais, D., & Turgeon, S. L. (2013). Exopolysaccharide-milk protein interactions in a
26 dairy model system simulating yoghurt conditions. *Dairy Science and Technology*, 93(3), 255–
27 271. <https://doi.org/10.1007/s13594-013-0121-x>
- 28 Girard, M., & Schaffer-Lequart, C. (2008). Attractive interactions between selected anionic
29 exopolysaccharides and milk proteins. *Food Hydrocolloids*, 22(8), 1425–1434.
30 <https://doi.org/10.1016/j.foodhyd.2007.09.001>
- 31 Glover, Z. J., Ersch, C., Andersen, U., Holmes, M. J., Povey, M. J., Brewer, J. R., & Simonsen, A. C.
32 (2019). Super-resolution microscopy and empirically validated autocorrelation image analysis
33 discriminates microstructures of dairy derived gels. *Food Hydrocolloids*, 90(December 2018),
34 62–71. <https://doi.org/10.1016/j.foodhyd.2018.12.004>
- 35 Hassan, A. N. (2008). ADSA foundation scholar award: Possibilities and challenges of
36 exopolysaccharide-producing lactic cultures in dairy foods. *Journal of Dairy Science*, 91(4),
37 1282–1298. <https://doi.org/10.3168/jds.2007-0558>
- 38 Hege, J., Palberg, T., & Vilgis, T. A. (2020). Interactions of different hydrocolloids with milk proteins.
39 *JPhys Materials*, 3(4). <https://doi.org/10.1088/2515-7639/aba2b7>
- 40 Hemar, Y., Tamehana, M., Munro, P. A., & Singh, H. (2001). Viscosity, microstructure and phase
41 behavior of aqueous mixtures of commercial milk protein products and xanthan gum. *Food*
42 *Hydrocolloids*, 15(4–6), 565–574. [https://doi.org/10.1016/S0268-005X\(01\)00077-7](https://doi.org/10.1016/S0268-005X(01)00077-7)
- 43 Jamil, T., Gissinger, J. R., Garley, A., Saikia, N., Upadhyay, A. K., & Heinz, H. (2019). Dynamics of

- 1 carbohydrate strands in water and interactions with clay minerals: Influence of pH, surface
2 chemistry, and electrolytes. *Nanoscale*, 11(23), 11183–11194.
3 <https://doi.org/10.1039/c9nr01867k>
- 4 Kayitmazer, A. B., Seyrek, E., Dubin, P. L., & Staggemeier, B. A. (2003). Influence of chain stiffness on
5 the interaction of polyelectrolytes with oppositely charged micelles and proteins. *Journal of*
6 *Physical Chemistry B*, 107(32), 8158–8165. <https://doi.org/10.1021/jp034065a>
- 7 Kruif, C. G. De, & Tuinier, R. (2001). *Polysaccharide protein interactions*. 15, 555–563.
- 8 Laneuville, S. I., & Turgeon, S. L. (2014). Microstructure and stability of skim milk acid gels containing
9 an anionic bacterial exopolysaccharide and commercial polysaccharides. *International Dairy*
10 *Journal*, 37(1), 5–15. <https://doi.org/10.1016/j.idairyj.2014.01.014>
- 11 Loeffler, M., Hilbig, J., Velasco, L., & Weiss, J. (2020). Usage of in situ exopolysaccharide-forming
12 lactic acid bacteria in food production: Meat products—A new field of application?
13 *Comprehensive Reviews in Food Science and Food Safety*, 19(6), 2932–2954.
14 <https://doi.org/10.1111/1541-4337.12615>
- 15 Lucey, J. A., & Singh, H. (1997). Formation and physical properties of acid milk gels: A review. *Food*
16 *Research International*, 30(7), 529–542. [https://doi.org/10.1016/S0963-9969\(98\)00015-5](https://doi.org/10.1016/S0963-9969(98)00015-5)
- 17 Lucey, John A. (2004). Cultured dairy products: An overview of their gelation and texture properties.
18 *International Journal of Dairy Technology*, 57(2–3), 77–84. [https://doi.org/10.1111/j.1471-](https://doi.org/10.1111/j.1471-0307.2004.00142.x)
19 [0307.2004.00142.x](https://doi.org/10.1111/j.1471-0307.2004.00142.x)
- 20 Lynch, K. M., Zannini, E., Coffey, A., & Arendt, E. K. (2018). *Lactic Acid Bacteria Exopolysaccharides in*
21 *Foods and Beverages : Isolation , Properties , Characterization , and Health Benefits*.
- 22 Marguerite, R. (2001). Relation between the molecular structure of some polysaccharides and
23 original properties in sol and gel states. *Food Hydrocolloids*, 15(4–6), 433–440.
- 24 Mende, S., Rohm, H., & Jaros, D. (2016). Influence of exopolysaccharides on the structure, texture,
25 stability and sensory properties of yoghurt and related products. *International Dairy Journal*, 52,
26 57–71. <https://doi.org/10.1016/j.idairyj.2015.08.002>
- 27 Metilli, L., Francis, M., Povey, M., Lazidis, A., Stephanie, M.-T., Ray, J., & Simone, E. (2020). Latest
28 advances in imaging techniques for characterizing soft, multiphasic food materials. *Advances in*
29 *Colloid and Interface Science*, 2019, 104265. <https://doi.org/10.1016/j.meegid.2020.104265>
- 30 Morris, G. A., Patel, T. R., Picout, D. R., Ross-Murphy, S. B., Ortega, A., Garcia de la Torre, J., &
31 Harding, S. E. (2008). Global hydrodynamic analysis of the molecular flexibility of
32 galactomannans. *Carbohydrate Polymers*, 72(2), 356–360.
33 <https://doi.org/10.1016/j.carbpol.2007.08.017>
- 34 Pugnali, L. A., Matia-Merino, L., & Dickinson, E. (2005). Microstructure of acid-induced caseinate
35 gels containing sucrose: Quantification from confocal microscopy and image analysis. *Colloids*
36 *and Surfaces B: Biointerfaces*, 42(3–4), 211–217. <https://doi.org/10.1016/j.colsurfb.2005.03.002>
- 37 Rinaudo, M., & Milas, M. (2000). Gellan gum, a bacterial gelling polymer. *Developments in Food*
38 *Science*, 41(C), 239–263. [https://doi.org/10.1016/S0167-4501\(00\)80012-6](https://doi.org/10.1016/S0167-4501(00)80012-6)
- 39 Robertson, C. (2012). Theory and practical recommendations for autocorrelation-based image
40 correlation spectroscopy. *Journal of Biomedical Optics*, 17(8), 080801.
41 <https://doi.org/10.1117/1.jbo.17.8.080801>
- 42 Savaiano, D. A., & Hutkins, R. W. (2021). Yogurt, cultured fermented milk, and health: A systematic
43 review. *Nutrition Reviews*, 79(5), 599–614. <https://doi.org/10.1093/nutrit/nuaa013>

- 1 Schefer, L., Adamcik, J., & Mezzenga, R. (2014). Unravelling secondary structure changes on
2 individual anionic polysaccharide chains by atomic force microscopy. *Angewandte Chemie -
3 International Edition*, 53(21), 5376–5379. <https://doi.org/10.1002/anie.201402855>
- 4 Silva, J. V. C., Legland, D., Cauty, C., Kolotuev, I., & Flourey, J. (2015). Characterization of the
5 microstructure of dairy systems using automated image analysis. *Food Hydrocolloids*, 44, 360–
6 371. <https://doi.org/10.1016/j.foodhyd.2014.09.028>
- 7 Sodini, I., Remeuf, F., Haddad, C., & Corrieu, G. (2004). The Relative Effect of Milk Base, Starter, and
8 Process on Yogurt Texture: A Review. *Critical Reviews in Food Science and Nutrition*, 44(2), 113–
9 137. <https://doi.org/10.1080/10408690490424793>
- 10 Sone, I., Hosoi, M., Geonzon, L. C., Jung, H., & Bernadette, F. (2022). Gelation and network structure
11 of acidified milk gel investigated at different length scales with and without addition of iota -
12 carrageenan. *Food Hydrocolloids*, 123(September 2021), 107170.
13 <https://doi.org/10.1016/j.foodhyd.2021.107170>
- 14 Super, B. J., & Bovik, A. C. (1991). Localized measurement of image fractal dimension using gabor
15 filters. *Journal of Visual Communication and Image Representation*, 2(2), 114–128.
16 [https://doi.org/10.1016/1047-3203\(91\)90002-W](https://doi.org/10.1016/1047-3203(91)90002-W)
- 17 Sworn, G., & Stouby, L. (2021). Gellan gum. In *Handbook of Hydrocolloids* (3rd ed.). Elsevier Ltd.
18 <https://doi.org/10.1016/b978-0-12-820104-6.00009-7>
- 19 Syrbe, A., Bauer, W. J., & Klostermeyer, H. (1998). Polymer science concepts in dairy systems - An
20 overview of milk protein and food hydrocolloid interaction. *International Dairy Journal*, 8(3),
21 179–193. [https://doi.org/10.1016/S0958-6946\(98\)00041-7](https://doi.org/10.1016/S0958-6946(98)00041-7)
- 22 Tamang, J. P., Cotter, P. D., Endo, A., Han, N. S., Kort, R., Liu, S. Q., Mayo, B., Westerik, N., & Hutkins,
23 R. (2020). Fermented foods in a global age: East meets West. *Comprehensive Reviews in Food
24 Science and Food Safety*, 19(1), 184–217. <https://doi.org/10.1111/1541-4337.12520>
- 25 Tan, Y. L., Ye, A., Singh, H., & Hemar, Y. (2007). Effects of biopolymer addition on the dynamic
26 rheology and microstructure of renneted skim milk systems. *Journal of Texture Studies*, 38(3),
27 404–422. <https://doi.org/10.1111/j.1745-4603.2007.00104.x>
- 28 Tiwari, S., Kavitate, D., Devi, P. B., & Halady Shetty, P. (2021). Bacterial exopolysaccharides for
29 improvement of technological, functional and rheological properties of yoghurt. *International
30 Journal of Biological Macromolecules*, 183, 1585–1595.
31 <https://doi.org/10.1016/j.ijbiomac.2021.05.140>
- 32 Tong, K., Xiao, G., Cheng, W., Chen, J., & Sun, P. (2018). Large amplitude oscillatory shear behavior
33 and gelation procedure of high and low acyl gellan gum in aqueous solution. *Carbohydrate
34 Polymers*, 199(July), 397–405. <https://doi.org/10.1016/j.carbpol.2018.07.043>
- 35 Torres, I. C., Amigo Rubio, J. M., & Ipsen, R. (2012). Using fractal image analysis to characterize
36 microstructure of low-fat stirred yoghurt manufactured with microparticulated whey protein.
37 *Journal of Food Engineering*, 109(4), 721–729. <https://doi.org/10.1016/j.jfoodeng.2011.11.016>
- 38 Tuinier, R., Van Casteren, W. H. M., Looijesteijn, P. J., Schols, H. A., Voragen, A. G. J., & Zoon, P.
39 (2001). Effects of structural modifications on some physical characteristics of
40 exopolysaccharides from *Lactococcus lactis*. *Biopolymers*, 59(3), 160–166.
41 [https://doi.org/10.1002/1097-0282\(200109\)59:3<160::AID-BIP1015>3.0.CO;2-V](https://doi.org/10.1002/1097-0282(200109)59:3<160::AID-BIP1015>3.0.CO;2-V)
- 42 Turgeon, S. L., & Laneuville, S. I. (2009). Protein + Polysaccharide Coacervates and Complexes. From
43 Scientific Background to their Application as Functional Ingredients in Food Products. In *Modern
44 Biopolymer Science* (First Edit). Elsevier Inc. <https://doi.org/10.1016/B978-0-12-374195->

1 0.00011-2

2 Weinbreck, F., Nieuwenhuijse, H., Robijn, G. W., & De Kruif, C. G. (2003). Complex Formation of
3 Whey Proteins: Exocellular Polysaccharide EPS B40. *Langmuir*, 19(22), 9404–9410.
4 <https://doi.org/10.1021/la0348214>

5 Williams, P. A., & Phillips, G. O. (2003). The use of hydrocolloids to improve food texture. In *Texture*
6 *in Food* (Vol. 1). Woodhead Publishing Limited. <https://doi.org/10.1533/9781855737082.2.251>

7 Zdunek, A., & Pieczywek, P. M. (2021). *The primary , secondary , and structures of higher levels of*
8 *pectin polysaccharides. September 2020*, 1101–1117. <https://doi.org/10.1111/1541-4337.12689>

9 Zhang, L., Folkenberg, D. M., Amigo, J. M., & Ipsen, R. (2016). Effect of exopolysaccharide-producing
10 starter cultures and post-fermentation mechanical treatment on textural properties and
11 microstructure of low fat yoghurt. *International Dairy Journal*, 53, 10–19.
12 <https://doi.org/10.1016/j.idairyj.2015.09.008>

13 Zhang, L., Folkenberg, D. M., Qvist, K. B., & Ipsen, R. (2015). Further development of a method for
14 visualisation of exopolysaccharides in yoghurt using fluorescent conjugates. *International Dairy*
15 *Journal*, 46, 88–95. <https://doi.org/10.1016/j.idairyj.2014.08.018>

16

17